

Magnetolectric excitations in multiferroic TbMnO₃ by Raman scattering

P. Rovillain, M. Cazayous, Y. Gallais, A. Sacuto, and M-A. Measson

Laboratoire Matériaux et Phénomènes Quantiques, UMR 7162 CNRS, Université Paris Diderot-Paris 7, 75205 Paris Cedex 13, France

H. Sakata

Department of Physics, Tokyo University of Science, 1-3 Kagurazaka, Shinjyuku-ku, Tokyo 162-8601, Japan

(Received 30 November 2009; published 18 February 2010)

Low-energy excitations in the multiferroic material TbMnO₃ have been investigated by Raman spectroscopy. Our observations reveal the existence of two peaks at 30 and 60 cm⁻¹. They are observed in the cycloidal phase below the Curie temperature but not in the sinusoidal phase, suggesting their magnetolectric origin. While the peak energies coincide with the frequencies of electromagnons measured previously by transmission spectroscopy, they show surprisingly different selection rules, with the 30 cm⁻¹ excitation enhanced by the electric field of light along the spontaneous polarization. The origins of the two modes are discussed under Raman and infrared selection rules considerations.

DOI: [10.1103/PhysRevB.81.054428](https://doi.org/10.1103/PhysRevB.81.054428)

PACS number(s): 77.80.B-, 75.25.-j, 75.50.Ee, 78.30.Hv

Multiferroics have both ferroelectricity and magnetism. For some of these materials, the magnetolectric coupling is especially strong and has attracted much attention for new spin-based device applications.¹ Substantial efforts have been dedicated to the research on the origin of the close coupling between the magnetic and electric orders. TbMnO₃ is one of the most intensively studied magnetolectric managanite among the frustrated magnets. The ferroelectricity in TbMnO₃ appears to be induced by an inverse Dzyaloshinski-Moriya interaction,^{2,3} even if the microscopic mechanism remains under debate.⁴ The strength of the magnetolectric coupling gives rise to dynamical effects like electromagnons,⁵ magnons with an electric dipole activity predicted by Baryakhtar and Chupis.⁶ Such excitations have been observed by far-infrared (IR) transmission.⁷⁻¹² This spectroscopy detects electromagnons for electric field of light \mathbf{E} parallel to the a axis of the crystal at around 2.5 meV (20–25 cm⁻¹) and 7.5 meV (60 cm⁻¹). Inelastic neutron measurements detect magnetic excitations at the same energies along the same crystallographic direction.¹³ From a theoretical point of view, Katsura *et al.*¹⁴ have proposed a model based on spins current to describe the electromagnons. This model can be regarded as an inverse Dzyaloshinskii-Moriya effect and predicts the observation of one electromagnon (20–25 cm⁻¹) with selection rule $\mathbf{E} \parallel a$ axis perpendicular to the bc plane in the spiral phase. A recent approach based on indirect Heisenberg exchange¹⁵ was proposed to explain the 60 cm⁻¹ electromagnon, while a calculation considering the cross-coupling between magnetostrictive and spin-orbit interactions¹⁶ was proposed to explain the both 20–25 and 60 cm⁻¹ excitations. Optical spectroscopies have different selection rules and the scattering processes involved in each spectroscopy should be differently sensitive to the electric dipole activity of the electromagnons. Among them, Raman scattering is an efficient probe for studying both magnetic (magnons) and ferroelectric (phonons) excitations and their mutual coupling.¹⁷⁻²⁰ However, up to now the electromagnon signature in TbMnO₃ has not been detected by Raman scattering.

Here, we investigate the magnetic excitations in TbMnO₃ through Raman measurements. Our study reveals magnons at

30 and 60 cm⁻¹ with the electric field of light $\mathbf{E} \parallel a$. The intensity of the magnon at 30 cm⁻¹ is enhanced with electric field $\mathbf{E} \parallel c$ while the magnon at 60 cm⁻¹ disappears and a strong band is detected at 128 cm⁻¹. The magnetic modes at 30 and 60 cm⁻¹ are only observed in the ferroelectric phase (cycloidal phase) which points out their electric-dipole activity.

TbMnO₃ single crystals were grown using the floating-zone method and crystallize in the orthorhombic symmetry of space group $Pbnm$.²¹ Below the Néel temperature $T_N = 42$ K the Mn magnetic moments order antiferromagnetically in an incommensurate sinusoidal wave with a modulation vector along the b axis (sinusoidal phase). At still lower temperature below $T_C = 28$ K, the spin wave modulation is transformed into a cycloid (cycloidal phase) with spins confined to the bc plane (Fig. 1). This transition is associated with the appearance of a spontaneous electric polarization P along the c axis. In this work, two samples with ac and bc planes have been investigated.

We have performed Raman measurements in a back-scattering geometry with a triple spectrometer Jobin Yvon T64000 using the 568 nm excitation line from a Ar⁺-Kr⁺

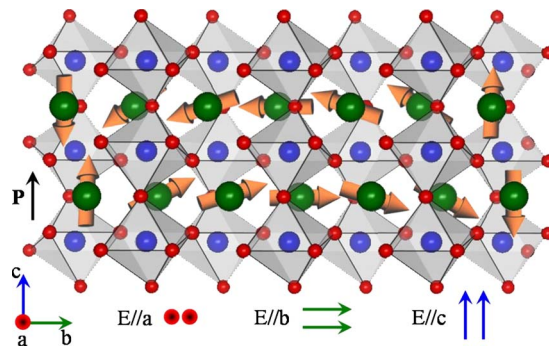


FIG. 1. (Color online) Structure of the orthorhombic TbMnO₃ crystal with the cycloid ordering of the Mn spins in the ferroelectric phase below T_C . The spins rotate in the bc plane around the a axis and propagate along the b direction. Parallel polarizations of the incident and scattered electric fields \mathbf{E} along the a , b , and c axes.

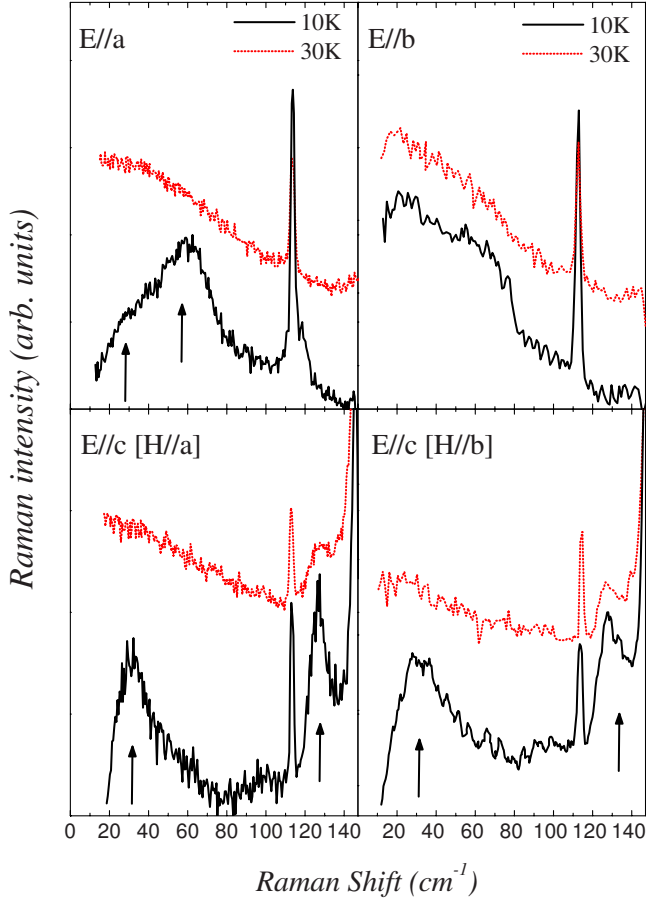


FIG. 2. (Color online) Raman response measured in the cycloidal (10 K) and sinusoidal phases (30 K) using different configurations for the electric \mathbf{E} and magnetic \mathbf{H} fields of light. Arrows show the magnon modes at 30, 60 cm^{-1} , and the band at 128 cm^{-1} .

mixed gas laser. Tiny signals have been obtained with other laser wavelengths. The high rejection rate of the spectrometer allows us to detect the magnons at frequencies below 100 cm^{-1} . The temperature dependences have been performed using an ARS closed-cycle He cryostat. Figure 1 shows the two configurations of light polarizations used. Incident and scattered lights are polarized along the same crystallographic axis.

Figure 2 shows the Raman response with different light polarizations in the cycloidal (10 K, below T_C) and sinusoidal phases (30 K, below T_N). (\mathbf{E} , \mathbf{H}) are the electric and magnetic fields of the light, respectively.

In $\mathbf{E}\parallel a$, a strong peak is observed at 60 cm^{-1} and a shoulder at 30 cm^{-1} (10 K) and both disappear at 30 K. The signature of these two peaks seems to be present in $\mathbf{E}\parallel b$ but with a weak intensity.

In $\mathbf{E}\parallel c$ ($\mathbf{H}\parallel a$ or $\mathbf{H}\parallel b$) polarization, the peak at 60 cm^{-1} disappears while the peak at 30 cm^{-1} grows up with a band at 128 cm^{-1} . Both have the same intensities in these two configurations. Since no phonon is expected under 100 cm^{-1} we believe that these two peaks are magnon modes. However, the origin of the two magnon modes is not obvious and is discussed below.

Figure 3 shows the temperature dependence of Raman

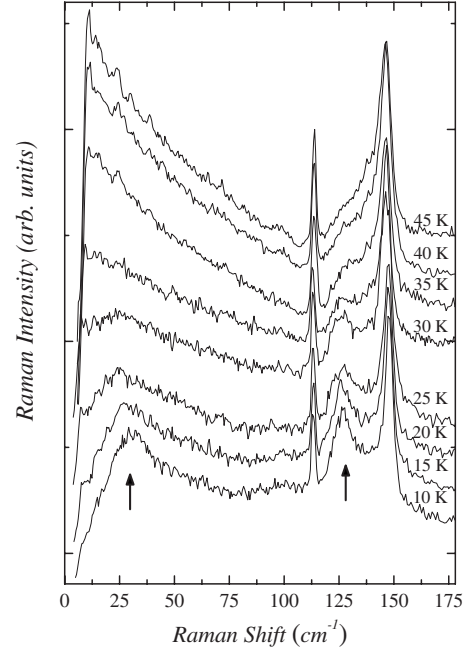


FIG. 3. Temperature-dependent Raman spectra in $\mathbf{E}\parallel c$ between 10 and 45 K. Observation of two peaks at 30 and 128 cm^{-1} and two phonons at 113 and 147 cm^{-1} .

spectra in the range 0–175 cm^{-1} from 10 to 45 K with $\mathbf{E}\parallel c$. The magnon mode at 30 cm^{-1} clearly disappears upon entering the sinusoidal phase ($T > 30$ K) whereas the band at 128 cm^{-1} is still observed in the collinear sinusoidal phase before finally vanishing at the Néel temperature ($T_N = 42$ K).

Figure 4(a) shows quantitatively that the frequency of the magnon mode at 30 cm^{-1} decreases down to the end of the cycloidal phase. The frequency of 60 cm^{-1} magnon [Fig. 4(b)] first increases from 10 K up to 20 K before decreasing until 30 K. These both magnetic excitations are only detected in the cycloidal phase whereas they should exist in the sinusoidal phase until the Néel temperature $T_N = 42$ K as expected for ordinary magnetic excitations. Our data show that both excitations have not a pure magnetic activity and are intimately related to the cycloidal phase below T_C .

Let us focus on the origin of these two magnetic peaks and on the Raman polarization selection rules. The peak at 60 cm^{-1} is assigned to a zone-edge magnon with an energy close to the zone-edge energy.^{10,11}

Previously measured at the same energy and with the same polarization $\mathbf{E}\parallel a$ by far-infrared transmission spectroscopy, this magnetic excitation has been identified as an electromagnon.^{7,9,10} Therefore, up to now only IR technique with its specific selection rules has been able to observe directly electromagnons. Raman measurements show that this magnetic excitation exists only in the cycloidal phase underlying the polar character of the zone-edge magnon.

Optical spectroscopies like Raman scattering probe dispersion branches close to the zero wave vector. The activation of 60 cm^{-1} zone-edge magnon can be explained by the alternation of the Heisenberg exchange interaction along b axis¹⁰ or by the coupling of this mode with the spontaneous polarization through the dynamical magnetoelectric field.¹⁶

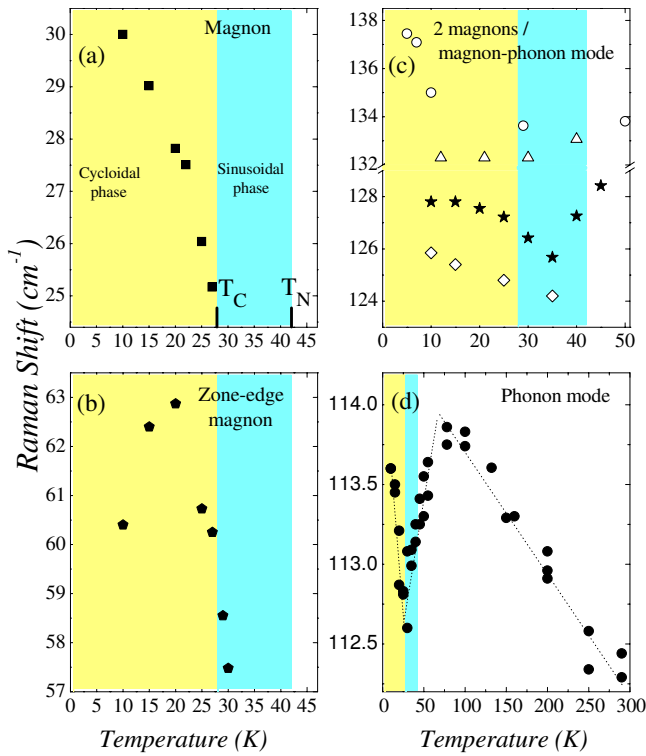


FIG. 4. (Color online) Our measurements (full symbol): frequency of the (a) 30 cm^{-1} (square), (b) 60 cm^{-1} magnons modes (hexagon), (c) 128 cm^{-1} band (star), and (d) 113 cm^{-1} phonon mode (circle) as a function of the temperature. (c) Open symbols: far-infrared data of Schmidt *et al.* (open circle) (Ref. 30) and Takahashi *et al.* (open triangle), (Ref. 9) and Raman measurements of Barath *et al.* (open diamond) (Ref. 28). The color zones define the cycloidal phase up to 28 K and the sinusoidal phase from 28 to 42 K. Lines are guide to the eyes.

The origin of the 30 cm^{-1} peak is more tricky. Two first simple explanations can be proposed. This peak might be assigned to zone-center magnon mode or Tb^{3+} f - f transitions. As mentioned before, Raman scattering probe dispersion branches close to the zero wave vector and this peak might be assigned a zone-center magnon mode. The Tb^{3+} f - f transitions should induce sharp peak in the Raman spectra. The peak at 30 cm^{-1} is too large (width= 20 cm^{-1}) to be associated with such transition. To the best of our knowledge, no Tb^{3+} f - f transition has been detected below 75 cm^{-1} .^{22–24} Moreover, this peak has been only observed below T_C .

The third explanation of the 30 cm^{-1} peak can be derived from comparison between several experimental techniques such as IR spectroscopy.

A broad peak has been already reported by IR between 20 and 25 cm^{-1} with $\mathbf{E}\parallel a$ and has been assigned to an electromagnon.^{7,9,12} Based on neutron measurements, this peak corresponds to a propagating mode of the spins out of the cycloidal plane.¹³ A stronger argument in favor of its electromagnon origin has been recently brought by Kida *et al.*²⁵ on DyMnO_3 and Aguilar *et al.*¹⁰ on TbMnO_3 . This excitation is only detected by far-infrared transmission using $\mathbf{E}\parallel a$ even when the magnetic field induces a transition from a spiral in the bc plane to the ab plane spiral.

From a theoretical point of view, the Dzyaloshinskii-Moriya interaction has been able to only predict the electromagnon at $20\text{--}25\text{ cm}^{-1}$ with a polar activity predicted for the electric field of light along the a axis.¹⁴ A recent model based on cross-coupling between magnetostriction and spin-orbit interactions can explain both the peak at $20\text{--}25$ and 60 cm^{-1} .¹⁶ In this model the mode at $20\text{--}25\text{ cm}^{-1}$ corresponds to an excitation combining the zone-edge magnon wave vector and twice the cycloid wave vector.

From an experimental point of view, infrared measurements show only the $20\text{--}25\text{ cm}^{-1}$ peak with $\mathbf{E}\parallel a$ whereas this peak (30 cm^{-1}) is enhanced with $\mathbf{E}\parallel c$ in Raman scattering. If the Raman mode observed at 30 cm^{-1} is the electromagnon observed by infrared at $20\text{--}25\text{ cm}^{-1}$, how to understand the distinct selection rules between IR and Raman?

First, it is well known that Raman scattering process are very different from the ones involved in IR whose peaks arise directly from the electric dipole activity of excitations. A Raman peak can arise from an excitation without an electric dipole activity. One can notice that the Raman selection rules have been established for magnon modes but up to now not for electromagnons.

Second, Raman and IR spectroscopies might be differently sensitive to the hybridization degree of electromagnons. We can notice that the 30 cm^{-1} mode measured by Raman scattering has a higher frequency compare to the electromagnons measured by infrared spectroscopies ($20\text{--}25\text{ cm}^{-1}$). The observation of this electromagnon at lower energy in infrared spectroscopy would suggest that infrared spectroscopy is more affected by the polar activity of the electromagnons than the Raman one. Magnetic field combined with infrared spectroscopy has been able to determine the electromagnon nature of the infrared peaks.¹⁰ Raman measurements have to be carried on the same direction.

In Fig. 3 the phonon modes at 113 and 148 cm^{-1} correspond to A_g -symmetry modes related to the displacements of the Tb^{3+} ions.^{26,27} The mode at 113 cm^{-1} is detected by Raman scattering in the two polarizations $\mathbf{E}\parallel a$ and $\mathbf{E}\parallel c$ whereas the mode at 148 cm^{-1} is only present in the polarization $\mathbf{E}\parallel c$. The behavior of the lowest phonon mode at 113 cm^{-1} is unusual [Fig. 4(d)] with a sharp frequency decreasing in the cycloidal phase followed by an increase up to 75 K before the usual frequency decrease at higher temperature due to the thermal expansion of the lattice.

The detection of phonon anomalies related to ferroelectricity is a quest to determine the microscopic mechanism involved and to explain how the spontaneous polarization appears.² Barath *et al.*²⁸ have observed the evolution of the phonon mode at 147 cm^{-1} under a magnetic field. More recently, no phonon anomaly has been found below 400 cm^{-1} by x-ray scattering. This suggests a nonconventional displacive ferroelectric transition in TbMnO_3 .²⁹ Here, we clearly observe a kink in the frequency of the c -polarized phonon at 113 cm^{-1} across T_C [Fig. 4(d)].

In Fig. 4(c), the frequency of the band at 128 cm^{-1} is shown with previously reported far-infrared and Raman measurements. This band decreases between 10 and 35 K and then increases up to 45 K. The measurements performed by Schmidt *et al.*³⁰ and Barath *et al.*²⁸ present the same decrease up to 35 K. The data of Takahashi *et al.*⁹ show a small discrepancy.

As already mentioned, this band disappears at the Néel temperature which underlines its magnetic character. The origin of this band has been discussed in previous papers and several interpretations have been proposed: magnon, a two-magnon scattering, or a magnon-phonon process.^{9,11,30} We discuss these interpretations in the light of our measurements and proposed an explanation based on crystal-field excitation (f - f transition).

First, this band cannot be associated with a one magnon process because we have measured the zone edge for magnetic excitations around 60 cm^{-1} . Second, the band at 128 cm^{-1} could be explained by the two-magnon scattering process, i.e., twice the magnon energy at 60 cm^{-1} .⁹ In the perfect crystals, magnon pairs are created with wave vectors q and $-q$ so that intensity is essentially proportional to the two-magnon density of states. The zone-edge magnon at 60 cm^{-1} is activated below T_C via the cycloidal order or its polar activity while the two-magnon mode is not inferred by T_C and is observed up to T_N . However, Lee *et al.*¹¹ have shown that the 128 cm^{-1} mode measured by IR spectroscopy only appears when the Tb^{3+} ion is included in RMnO_3 compounds. The two-magnon scattering process seems to be unlikely.

Third, we consider the one-magnon+one-phonon scenario.^{31,32} One phonon is produced simultaneously in addition to the two spin flip. In the range 10–45 K, the temperature dependence of the 128 cm^{-1} band [Fig. 4(c)] is similar to the one of the 113 cm^{-1} phonon mode [Fig. 4(d)]. This observation suggest that the band at 128 cm^{-1} might arise from a magnon-phonon scattering process involving the

magnon at 30 cm^{-1} and the phonon at 113 cm^{-1} . In $\text{Eu}_{0.75}\text{Y}_{0.25}\text{MnO}_3$, the magnon mode is at 25 cm^{-1} and the phonon is at 120 cm^{-1} .³³ However, no band around 145 cm^{-1} resulting from a one-magnon+one-phonon process is observed. The band at 128 cm^{-1} seems to be only related to the Tb compounds. This observation is not in favor of a one-magnon+one-phonon process.

The measurements performed by Lee *et al.*¹¹ and Aguilar *et al.*³³ show that the absorption band observed by infrared spectroscopy around 128 cm^{-1} is not present in other RMnO_3 . This band seems to be related to Tb ions and could be ascribed to a Tb^{3+} f - f transition. In this interpretation, the similar temperature dependence of the 128 cm^{-1} band and the 113 cm^{-1} phonon mode frequencies can be understood as a coupling between the Tb^{3+} f - f transition and the displacement of the Tb^{3+} ions.

In summary, our Raman observations reveal two magnetic excitations at 30 and 60 cm^{-1} with light polarization $\mathbf{E} \parallel a$. Surprisingly, our measurements show that the 30 cm^{-1} mode is enhanced with a light electric field along the spontaneous polarization (c axis). Both modes are only present in the cycloidal phase below T_C underlying their unusual magnetic character. The mode at 60 cm^{-1} is interpreted as the zone-edge magnon-phonon hybridization with the phonon part describing the electric polarization parallel to a . The Raman selection rules for the 30 cm^{-1} excitation show its complex origin.

The authors would like to thank R. de Sousa for helpful discussions and for a critical reading of the manuscript.

-
- ¹H. Béa, M. Gajek, M. Bibes, and A. Barthelemy, *J. Phys.: Condens. Matter* **20**, 434221 (2008).
- ²H. Katsura, N. Nagaosa, and A. V. Balatsky, *Phys. Rev. Lett.* **95**, 057205 (2005).
- ³I. A. Sergienko and E. Dagotto, *Phys. Rev. B* **73**, 094434 (2006).
- ⁴I. A. Sergienko, C. Sen, and E. Dagotto, *Phys. Rev. Lett.* **97**, 227204 (2006).
- ⁵A. Cano, *Phys. Rev. B* **80**, 180416(R) (2009).
- ⁶V. G. Baryakhtar and I. E. Chupis, *Sov. Phys. Solid State* **11**, 2628 (1970).
- ⁷A. Pimenov, A. Mukhin, V. Ivanov, V. Travkin, A. Balbashov, and A. Loidl, *Nat. Phys.* **2**, 97 (2006).
- ⁸A. B. Sushkov, R. V. Aguilar, S. Park, S-W. Cheong, and H. D. Drew, *Phys. Rev. Lett.* **98**, 027202 (2007).
- ⁹Y. Takahashi, N. Kida, Y. Yamasaki, J. Fujioka, T. Arima, R. Shimano, S. Miyahara, M. Mochizuki, N. Furukawa, and Y. Tokura, *Phys. Rev. Lett.* **101**, 187201 (2008).
- ¹⁰R. Valdés Aguilar, M. Mostovoy, A. B. Sushkov, C. L. Zhang, Y. J. Choi, S-W. Cheong, and H. D. Drew, *Phys. Rev. Lett.* **102**, 047203 (2009).
- ¹¹J. S. Lee, N. Kida, S. Miyahara, Y. Takahashi, Y. Yamasaki, R. Shimano, N. Furukawa, and Y. Tokura, *Phys. Rev. B* **79**, 180403(R) (2009).
- ¹²A. Pimenov, A. Shuvaev, A. Loidl, F. Schrettle, A. A. Mukhin, V. D. Travkin, V. Yu. Ivanov, and A. M. Balbashov, *Phys. Rev. Lett.* **102**, 107203 (2009).
- ¹³D. Senff, P. Link, K. Hradil, A. Hiess, L. P. Regnault, Y. Sidis, N. Aliouane, D. N. Argyriou, and M. Braden, *Phys. Rev. Lett.* **98**, 137206 (2007).
- ¹⁴H. Katsura, A. V. Balatsky, and N. Nagaosa, *Phys. Rev. Lett.* **98**, 027203 (2007).
- ¹⁵A. B. Sushkov, M. Mostovoy, R. Valdes Aguilar, S-W. Cheong, and H. D. Drew, *J. Phys.: Condens. Matter* **20**, 434210 (2008).
- ¹⁶M. P. V. Stenberg and R. de Sousa, *Phys. Rev. B* **80**, 094419 (2009).
- ¹⁷M. Cazayous, Y. Gallais, A. Sacuto, R. de Sousa, D. Lebeugle, and D. Colson, *Phys. Rev. Lett.* **101**, 037601 (2008).
- ¹⁸M. K. Singh, R. Katiyar, and J. F. Scott, *J. Phys.: Condens. Matter* **20**, 252203 (2008).
- ¹⁹J. F. Scott, M. K. Singh, and R. Katiyar, *J. Phys.: Condens. Matter* **20**, 322203 (2008); **20**, 425223 (2008).
- ²⁰P. Rovillain, M. Cazayous, Y. Gallais, A. Sacuto, R. P. S. M. Lobo, D. Lebeugle, and D. Colson, *Phys. Rev. B* **79**, 180411(R) (2009).
- ²¹J. Blasco, C. Ritter, J. Garcia, J. M. de Teresa, J. Pérez-Cacho, and M. R. Ibarra, *Phys. Rev. B* **62**, 5609 (2000).
- ²²J. A. Koningstein and G. Schaack, *Phys. Rev. B* **2**, 1242 (1970).
- ²³D. Boal, P. Grunberg, and J. A. Koningstein, *Phys. Rev. B* **7**, 4757 (1973).
- ²⁴V. V. Eremin, V. S. Kurnosov, A. V. Peschanski, V. I. Fomin,

- and E. N. Khats'ko, *Low Temp. Phys.* **33**, 915 (2007).
- ²⁵N. Kida, Y. Ikebe, Y. Takahashi, J. P. He, Y. Kaneko, Y. Yamasaki, R. Shimano, T. Arima, N. Nagaosa, and Y. Tokura, *Phys. Rev. B* **78**, 104414 (2008).
- ²⁶L. Martin-Carron, A. de Andres, M. J. Martinez-Lope, M. T. Casais, and J. A. Alonso, *Phys. Rev. B* **66**, 174303 (2002).
- ²⁷S. Venugopalan, Mitra Dutta, A. K. Ramdas, and J. P. Remeika, *Phys. Rev. B* **31**, 1490 (1985).
- ²⁸H. Barath, M. Kim, S. L. Cooper, P. Abbamonte, E. Fradkin, I. Mahns, M. Rubhausen, N. Aliouane, and D. N. Argyriou, *Phys. Rev. B* **78**, 134407 (2008).
- ²⁹R. Kajimoto, H. Sagayama, K. Sasai, T. Fukuda, S. Tsutsui, T. Arima, K. Hirota, Y. Mitsui, H. Yoshizawa, A. Q. R. Baron, Y. Yamasaki, and Y. Tokura, *Phys. Rev. Lett.* **102**, 247602 (2009).
- ³⁰M. Schmidt, Ch. Kant, T. Rudolf, F. Mayr, A. A. Mukhin, A. M. Balbashov, J. Deisenhofer, and A. Loidl, *Eur. Phys. J. B* **71**, 411 (2009).
- ³¹D. J. Lockwood, G. Mischler, I. W. Johnstone, and M. C. Schmidt, *J. Phys. C* **12**, 1955 (1979).
- ³²J. I. Takahashi, K. Hagia, K. Kohn, Y. Tanabe, and E. Hanamura, *Phys. Rev. Lett.* **89**, 076404 (2002).
- ³³R. Valdés Aguilar, A. B. Sushkov, C. L. Zhang, Y. J. Choi, S-W. Cheong, and H. D. Drew, *Phys. Rev. B* **76**, 060404(R) (2007).